Journal of Power Sources 198 (2012) 90–94

Contents lists available at SciVerse ScienceDirect

Journal of Power Sources

journal homepage: www.elsevier.com/locate/jpowsour

Short communication

Extended reaction zone of $La_{0.6}Sr_{0.4}Co_{0.2}Fe_{0.8}O_3$ cathode for solid oxide fuel cell

Zigui Lu*, John Hardy, Jared Templeton, Jeffry Stevenson

Energy and Environmental Directorate, Pacific Northwest National Laboratory, Richland, WA 99352, USA

ARTICLE INFO

Article history:
Received 1 July 2011
Received in revised form 26 August 2011
Accepted 9 September 2011
Available online 16 September 2011

Keywords:
Oxygen reduction reaction
Cathode thickness
Extended reaction zone
Electrochemical impedance spectroscopy

ABSTRACT

The oxygen reduction reaction can only proceed at locations where gas, electronic conductor, and an oxygen ion conductor meet. Although the extension of the reaction zone beyond the traditional so-called triple-phase-boundary (TPB) is widely accepted for a mixed ionically and electronically conductive cathode, work in this area has yet to reach a consensus on how far the reaction zone can be extended. In this study, anode-supported fuel cells with a variety of LSCF cathode thicknesses were fabricated and tested in two cathode environments, flowing oxygen and flowing air. In flowing oxygen, the cell performance increased with LSCF cathode thickness over the entire range investigated (from 5 to 33 μm) because of the increased number of reaction sites. In flowing air, the cell performance also increased with the LSCF cathode thickness from 5 to 13 μm, but then remained almost constant with further increase in cathode thickness due to depletion of oxygen beyond a certain thickness.

Published by Elsevier B.V.

1. Introduction

The oxygen reduction reaction at the cathode of a solid oxide fuel cell (SOFC) requires the simultaneous involvement of oxygen molecules, electrons, and oxygen ions and therefore can only proceed at locations where gas, electronic conductor, and an oxygen ion conductor meet. For porous SOFC cathode materials that are purely electronic conductors like the widely used $La_{1-x}Sr_xMnO_3$ (LSM), the reaction zone is generally confined to a region close to the interface of the cathode and the electrolyte, leading to limited cathode performance [1]. Significant improvement in cathode performance has been realized by adding an ionically conductive phase, such as yttria stabilized zirconia (YSZ), into the electronically conductive phase to form a composite [1–5], or by using a single-phase material with mixed ionic and electronic conductivity, such as $La_{1-x}Sr_xCo_{1-y}Fe_yO_3$ (LSCF) or $Sm_{0.5}Sr_{0.5}CoO_3$ as the cathode [6,7]. In these scenarios, the reaction zone can be extended into the bulk of the cathode, where oxygen molecules can be reduced to oxygen ions and then transported to the electrolyte through solid-state bulk diffusion, because of the ionic conductivity of the cathode.

Although the extension of the reaction zone is widely accepted in the fuel cell community for mixed conducting cathodes, work in this area has yet to reach a consensus on how far the reaction zone can be extended. Numerous models have been constructed to better understand the performance of porous mixed conductive electrodes, among which several have received wide attention [8–12]. In a model proposed by Adler et al. [9], it is predicted that for the best cathode materials, extension of the reaction zone beyond the interface of the cathode and the electrolyte is typically limited to a few micrometers. Other experimental results by Kenjo et al. on $Pt+(Bi_2O_3)_{0.7}(Er_2O_3)_{0.3}$ (EDB) composite cathode [12] or by Koyama et al. on $Sm_{0.5}Sr_{0.5}CoO_3$ mixed conductor cathode [7] showed much larger reaction zones.

The difference in the cathode reaction zone might result from the differences in chemical and physical properties of the cathode materials (bulk diffusion coefficient, surface exchange coefficient, interfacial resistance, etc.) and micro-structure of the cathode (particle and pore size, porosity), as well as the testing conditions. Two experimental artifacts in electrochemical measurements can also affect the interpretation of the experimental results, as pointed out by Adler [13]: (1) polarization resistance caused by gas-phase diffusion, and (2) artifacts related to the cell geometry. Recently, it was discovered from electrochemical impedance spectroscopy that concentration polarization originating from oxygen gas diffusion contributes significantly to the total polarization of the cathode reaction especially at high current densities, even with air flow at the cathode [14]. By flowing pure oxygen at the cathode, the concentration polarization can be eliminated.

In this study, the effect of the LSCF cathode thickness on the polarization resistance in both flowing oxygen and air was investigated. It was expected that with elimination of concentration polarization by flowing oxygen to the cathode, additional light

* Corresponding author at: Praxair, Inc., 175 East Park Drive, Tonawanda, NY 14150, USA. Tel.: +1 716 879 2569; fax: +1 716 879 7567.
E-mail address: zigui_lu@praxair.com (Z. Lu).

0378-7753/$ – see front matter. Published by Elsevier B.V.
doi:10.1016/j.jpowsour.2011.09.020

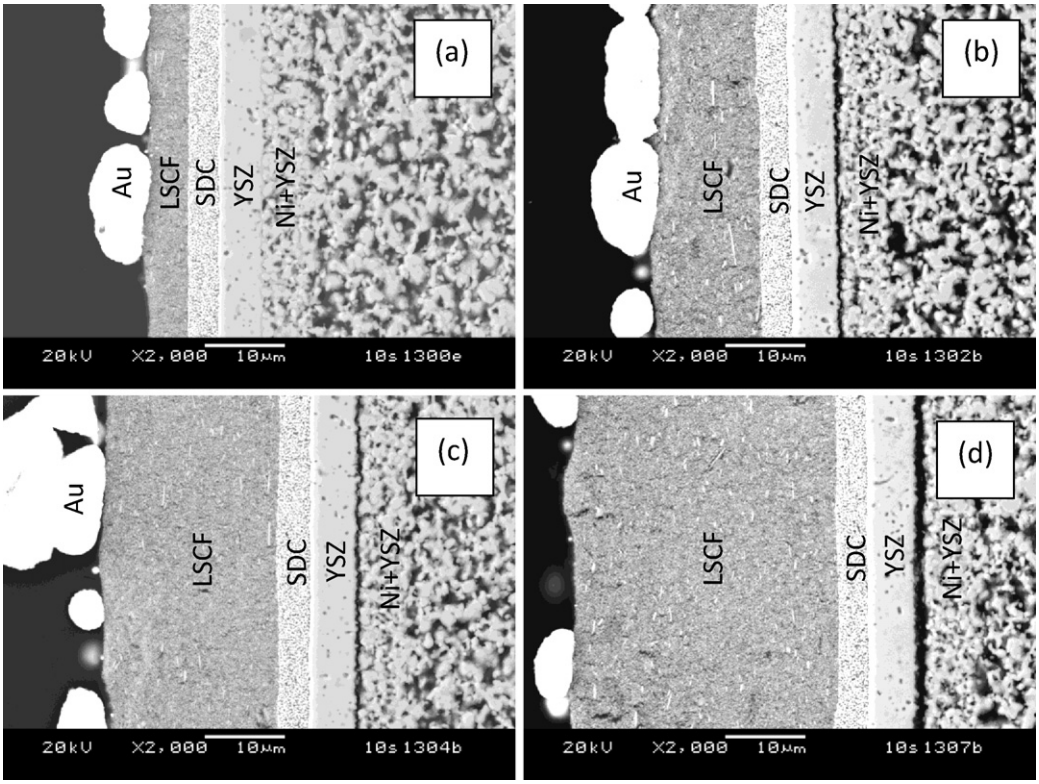

Fig. 1. Cross-sections of fuel cells with various LSCF cathode thicknesses: (a) 5 μm; (b) 13 μm; (c) 22 μm; and (d) 33 μm.

would be shed on how far the cathode reaction zone can be extended. On the other hand, by measuring the polarization resistance in air, the concentration resistance with different cathode thicknesses was also evaluated, in order to provide helpful insights into optimizing the microstructure of the cathode to achieve better gas delivery.

2. Experimental

Ni + YSZ anode-supported YSZ bi-layers were fabricated by a tape-casting and lamination process, described in more detail elsewhere [15]. A $Sm_{0.2}Ce_{0.8}O_{1.9}$ (SDC) interlayer was applied between the YSZ electrolyte and the $La_{0.6}Sr_{0.4}Co_{0.2}Fe_{0.8}O_3$ (LSCF) cathode to block potential interdiffusion and chemical reaction between these two components. The SDC interlayer was fabricated by screen-printing SDC ink on the YSZ electrolyte and sintering at 1200 °C for 2 h. The SDC ink was made by mixing SDC powder (Praxair, d_{50} = 0.2 μm) with a binder (V-006, Heraeus) on a three-roll mill. The solid loading of the ink was about 38% by weight. The fired SDC layer was about 4 μm thick and contained about 25% porosity, as measured from the weight and volume of this layer. LSCF (Praxair) was used as the cathode material. The as-received powder (d_{50} = 1.0 μm) was attrition milled to reduce the particle size to about 0.3 μm. The LSCF cathode was fabricated by screen-printing LSCF ink onto the SDC interlayer and sintering at 900 °C for 2 h. Fuel cells with a series of LSCF cathode thicknesses from 5 μm to 33 μm were fabricated by controlling the number of prints of the LSCF cathode, with each print yielding about 4 μm in thickness on average. In the case of a fuel cell with multiple cathode prints, the cathode ink was dried in an oven at 70 °C after each print and fired at 900 °C for 2 h. Au was used as the cathode current collector to exclude any possible contribution to the cell performance since Au does not have any catalytic activity toward the cathode reaction. The Au current collector was fabricated by screen-printing Au ink on the LSCF cathode and firing at 850 °C for 2 h. The thickness of Au current collector is about 5 μm and the active cathode area is 2 cm^2 in this study.

The fuel cells were sealed to alumina tubes using a glass seal, and *I–V* and impedance spectra were recorded using a Solartron 1470 Multistat coupled with a Solartron 1255 frequency response analyzer. EIS was performed under various operating voltages in both oxygen and air. When performed under an operating voltage, the cell was held at that voltage for 10 min before the impedance measurement was executed. Moist hydrogen with a flow rate of 200 sccm was supplied to the anode and air or oxygen with a flow rate of 500 sccm was supplied to the cathode. After testing, the fuel cells were observed under scanning electron microscopy (SEM) (JEOLJSM-5900LV) for cross-sectional views.

3. Results and discussion

Fig. 1 shows the cross-sections of fuel cells after testing with LSCF cathode thicknesses from 5 μm to 33 μm. The LSCF cathodes had a very fine structure with particle and pore sizes that were less than 1 μm in diameter after sintering at 900 °C for 2 h. It is noted that, to enable direct comparison between the fuel cells with different cathode thicknesses, all the anode/electrolyte bi-layers were made from the same tape and all the cell components were fabricated by the same procedure, so that any change in cell performance can be safely attributed to the change in cathode thickness. Indeed, all the other cell components except the cathode exhibited very similar microstructure and thickness, as shown in Fig. 1. The delamination between the Ni + YSZ anode and YSZ electrolyte for some of the cells observed in the SEM images (Fig. 1b–d) probably occurred during SEM sample preparation due to the shrinkage of the resin during curing. The similar ohmic resistance between the cells with different cathode thicknesses and the small change in

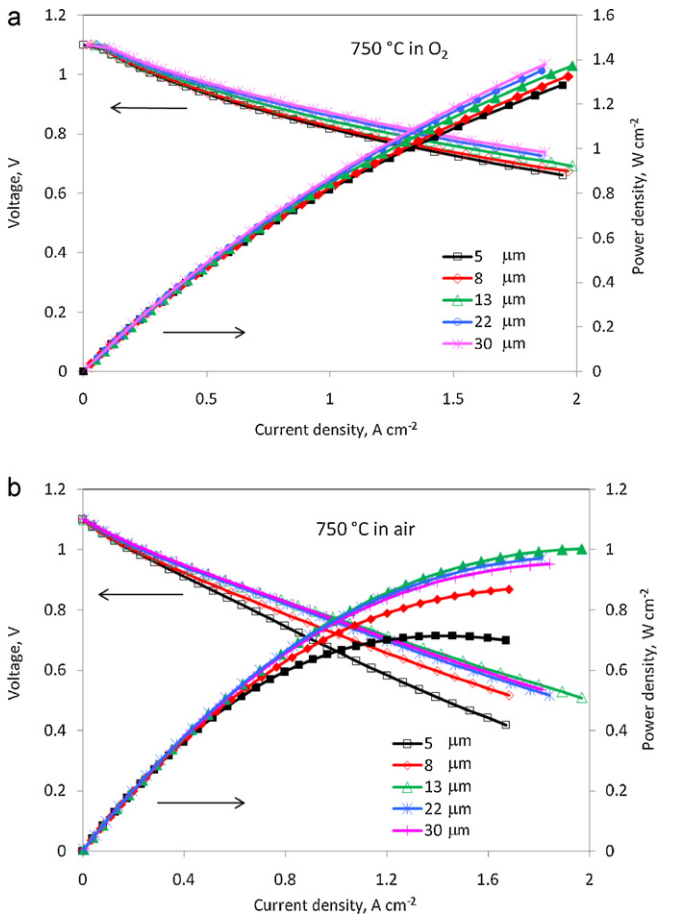

Fig. 2. *I–V* curves of fuel cells with various cathode thicknesses at 750 °C in (a): flowing oxygen and (b): flowing air.

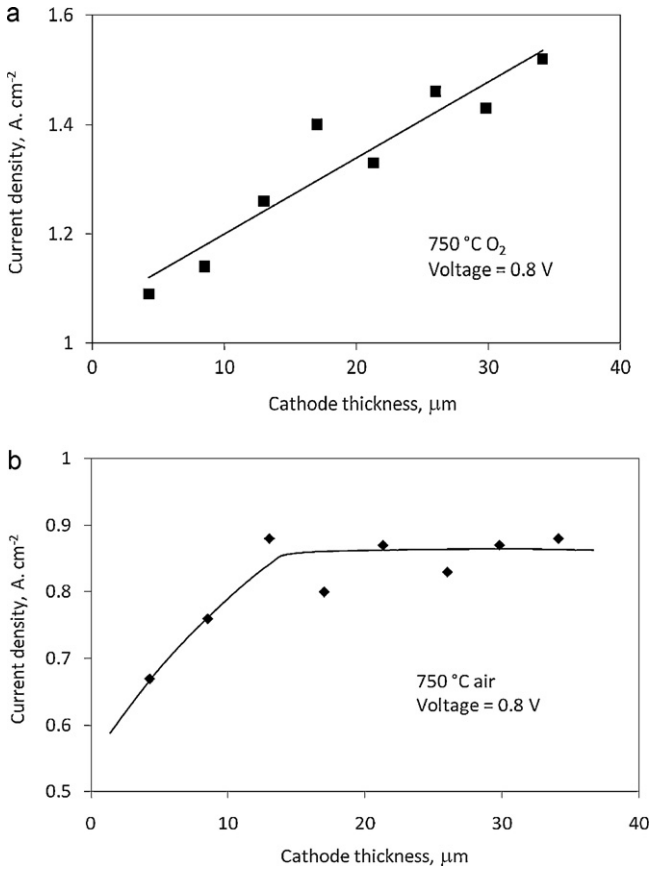

Fig. 3. Current densities of fuel cells at 0.8 V and 750 °C as a function of LSCF cathode thickness in (a) flowing oxygen and (b) flowing air.

ohmic resistance over time is a good indication that no significant delamination occurred during cell measurement.

Fig. 2 shows the *I–V* curves of the fuel cells with various LSCF cathode thicknesses at 750 °C in flowing oxygen (Fig. 2a) and flowing air (Fig. 2b). In flowing oxygen, the power density of the fuel cells increased with the LSCF cathode thickness in the entire range investigated. In flowing air, the power density of the fuel cells also increased with the LSCF cathode thickness from 5 μm to 13 μm, but then remained relatively constant with further increase in cathode thickness. The change in cell performance is more clearly visualized in the change of current density at 0.8 V as a function of LSCF cathode thickness, shown in Fig. 3. In flowing oxygen (Fig. 3a), the current density increased from 1.06 to 1.52 A cm^{-2} as the LSCF thickness increased from 5 μm to 33 μm; while in flowing air (Fig. 3b), the current density increased from 0.67 to 0.88 A cm^{-2} as the cathode thickness increased from 5 μm to 13 μm and then reached a plateau with further increase in cathode thickness.

Fig. 4 shows the impedance spectra of cells with different cathode thicknesses in flowing oxygen (Fig. 4a) and flowing air (Fig. 4b). Open circuit voltages (OCVs) of 1.10 V in air and 1.14 V in oxygen were typically observed for these cells. Electrochemical impedance measurements were performed at voltages of 1.00 and 1.05 V in air and oxygen, respectively, slightly lower than the OCVs to allow low current densities through the cells. At low current density, the polarization is governed by the activation over-potential, which arises from the kinetics of charge transfer reactions across interfaces. From the impedance spectra, both the ohmic and polarization resistances of the fuel cells with different cathode thicknesses were obtained by fitting the curves with an equivalent circuit, shown in Fig. 5. The ohmic resistances of the fuel cells with cathode thicknesses of 16 and 26 μm were a little smaller than those of the others in both oxygen and air. The reason for the smaller ohmic resistance of these two cells is unclear. All the other cells showed very similar ohmic resistance, which is reasonable considering the high electronic conductivity and small thickness of the cathode. The slight difference in the ohmic resistance of the cells in air and in oxygen was possibly due to the degradation of cells during the electrochemical measurement.

Three arcs appeared in the EIS in both flowing air and flowing oxygen, designated as high, medium, and low arc with peak frequencies of 1k, 10, and 0.5 Hz, respectively. The contribution of each arc to the total polarization resistance was obtained by fitting the curves with an equivalent circuit and plotted as a function of cathode thickness in Fig. 6. Good fitting was achieved for all the fuel cells with various LSCF thicknesses; examples of the fitting results for the 5 μm LSCF cell in O_2 and air are included in Fig. 5. From Fig. 6, as the cathode thickness increased, the contribution from the high frequency arc decreased, while those of the medium and low arcs remained almost constant. Since the EIS measurements were performed under constant voltages, the current passing through the cell will increase with the increased cathode thickness (due to the increase in cell performance), which might have an impact on the polarization resistance of the fuel cells. However, as demonstrated in the previous study [14], if the decrease in polarization resistance was due to the increase in current density, all the three arcs should decrease with similar magnitude, which is not the case in this study. Therefore, the fact that the decrease in size only occurs for the high frequency arc is attributed to the increase in cathode thickness, i.e. the increase in reaction sites.

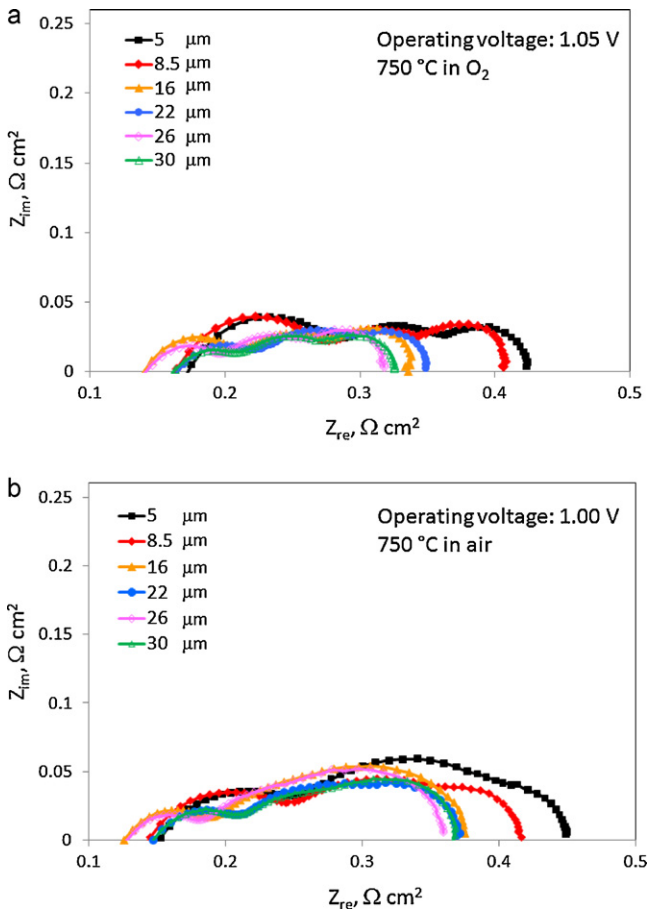

Fig. 4. Impedance spectra of fuel cells at with various LSCF cathode thicknesses at 750 °C in (a) flowing oxygen and (b) flowing air.

In flowing air, the high frequency arc also decreased as the cathode thickness increased from 5 to 13 μm and then remained almost constant with further increase in cathode thickness, shown in Fig. 6b. The middle and low frequency arcs overlapped and were difficult to separate from each other by fitting the curves. Therefore, the contributions of these two arcs were plotted together and also included in Fig. 6b. The contributions from the middle and low frequency arcs were almost constant at all cathode thicknesses, similar to those in flowing oxygen. The low frequency arc is possibly related to the gas-phase diffusion of oxygen from outside of the cathode to the reaction site, according to the previous study [14].

In flowing oxygen, since there is no limitation for oxygen diffusion, all the polarization resistance from the cathode should be attributed to the oxygen reduction reaction itself, such as absorption/adsorption of oxygen molecules on the surface of the cathode, the charge transfer process, and the transport of oxygen ion through the cathode. Since the LSCF cathode is a mixed conductor with electronic conductivity of 300 S cm^{-1} and ionic conductivity from 10^{-3} to 0.05 S cm^{-1} at 750 °C [16–18], the oxygen reduction reaction can occur at surface sites throughout the thickness of the cathode rather than just at TPB. Therefore, the high frequency arc is possibly related to the charge transfer process which requires the presence of oxygen gas, electrons, and oxygen vacancies simultaneously. The decrease in size of the high frequency arc with increase in cathode thickness indicates that in flowing oxygen, the charge transfer process is the rate determining step of the oxygen reduction reaction. Increasing the thickness of the cathode provides more reaction sites for the oxygen reaction and therefore decreases the polarization resistance. The monotonic increase of current density with cathode thickness indicates that the active reaction zone is still beyond the thickness investigated in this study. On the other hand, in flowing air, due to diffusion limitations, the outer part of the cathode, about 13 μm in this study, contribute more significantly to the oxygen reduction reaction than the rest of the thickness due to depletion of oxygen beyond a certain cathode thickness. The rest of the cathode acts more as conducting layer for transporting the oxygen ions which were reduced in the upper portion of the cathode.

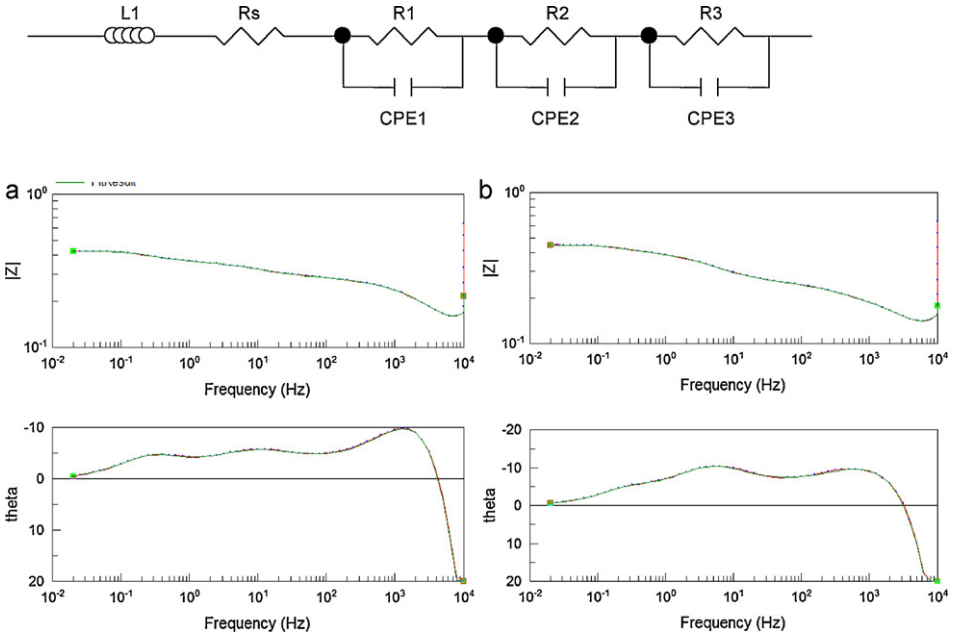

Fig. 5. The equivalent circuit used to fit the electrochemical impedance spectra in Fig. 4 and two examples of the fitting (colored lines) results for 5 μm LSCF fuel cell in (a) O_2 and (b) air.

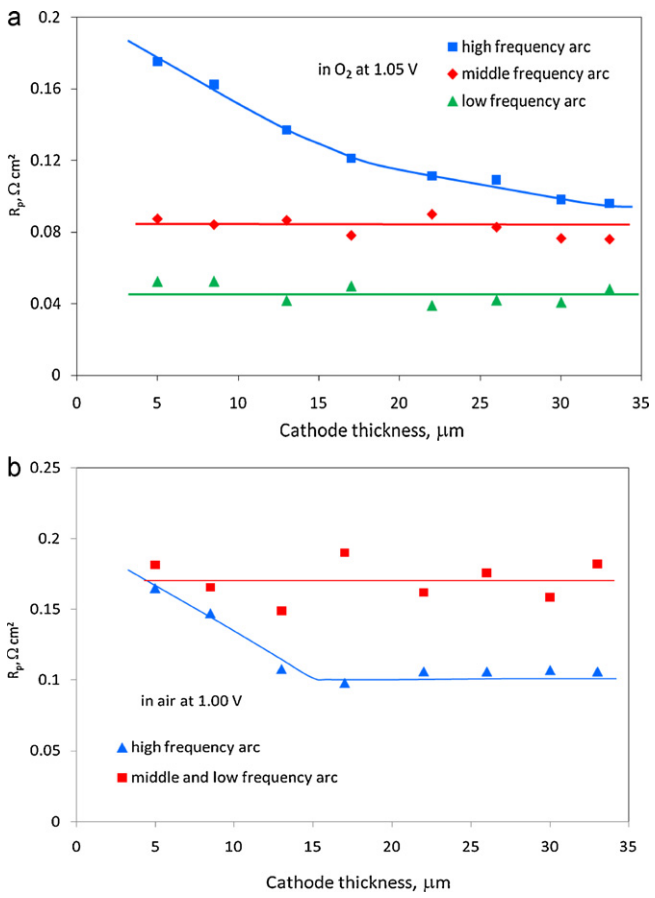

Fig. 6. Contributions of low, middle, and high frequency arcs to the total polarization resistance of cells with various cathode thicknesses at 750 °C in (a) oxygen and (b) air. Results obtained by fitting EIS in Fig. 4.

Plotting the polarization resistances of the high frequency arc against the cathode thickness, a linear relationship was established between the cathode thickness and the reciprocal of this component of polarization resistance, as shown in Fig. 7. The linear relationship between the reciprocal of the polarization resistance contributed by the high frequency arc and the cathode thickness indicates that the high frequency arc is probably related to the charge transfer process which can only occur at locations where oxygen molecules, electrons, and oxygen ions meet. Increasing the LSCF cathode thickness increases the number of reaction sites and therefore decreases the polarizations resistance

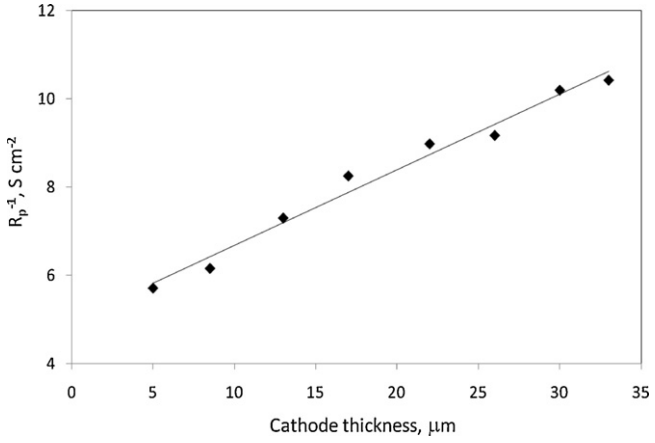

Fig. 7. The reciprocal of the polarization resistance contributed from the high frequency arc of EIS performed under 1.05 V in flowing oxygen as a function of cathode thicknesses at 750 °C.

4. Conclusion

The effect of LSCF cathode thickness on the performance of anode-supported SOFC was investigated in both flowing oxygen and flowing air. In flowing oxygen, the cell performance increased with LSCF cathode thickness in the entire range investigated (from 5 to 33 μm); in flowing air, the cell performance also increased as the LSCF cathode thickness increased from 5 to 13 μm, then it remained almost constant with further increase in cathode thickness. In flowing oxygen, since there was no oxygen diffusion limitation, the polarization resistance of oxygen reduction reaction is mainly determined by the charge transfer process, which occurs only at sites where oxygen gas, electrons, and oxygen vacancies are simultaneously present. Increase in the cathode thickness increases these active sites and therefore reduces the polarization resistance of the cathode. In flowing air, due to oxygen diffusion limitation, only a certain layer from the surface of the cathode is active in oxygen reduction reaction, while the rest of the underlying layer only acts as conducting layer to transport the reduced oxygen ions. It is expected that if the diffusion of oxygen in the LSCF cathode can be improved through optimization of cathode microstructure, the performance of the fuel cell can be much enhanced in air with optimal cathode thickness.

Acknowledgements

This work is supported by Department of Energy (DOE) Solid-state Energy Conversion Alliance (SECA) Core Technology Program. The authors would like to acknowledge James Coleman and Shelley Carlson for the SEM work.

References

[1] E.P. Murray, T. Tsai, S.A. Barnett, Solid State Ionics 110 (1998) 235.
[2] M.J.L. Ostergard, C. Clausen, C. Bagger, M. Mogensen, Electrochim. Acta 40 (1995) 1971.
[3] M.J. Jorgensen, M. Mogensen, J. Electrochem. Soc. 148 (2001) A433.
[4] E.P. Murray, M.J. Sever, S.A. Barnett, Solid State Ionics 148 (2002) 27.
[5] F. Zhao, A.V. Virkar, J. Power Sources 141 (2005) 79.
[6] A. Mai, V.A.C. Haanappel, S. Uhlenbruck, F. Tietz, D. Stover, Solid State Ionics 176 (2005) 1341.
[7] M. Koyama, C.J. Wen, T. Masuyama, J. Otomo, H. Fukunaga, K. Yamada, K. Eguchi, H. Takahashi, J. Electrochem. Soc. 148 (2001) A795.
[8] H. Fukunaga, M. Ihara, K. Sakaki, K. Yamada, Solid State Ionics 86–8 (1996) 1179.
[9] S.B. Adler, J.A. Lane, B.C.H. Steele, J. Electrochem. Soc. 143 (1996) 3554.
[10] R. O'Hayre, D.M. Barnett, F.B. Prinz, J. Electrochem. Soc. 152 (2005) A439.
[11] X.H. Deng, A. Petric, J. Power Sources 140 (2005) 297.
[12] T. Kenjo, S. Osawa, K. Fujikawa, J. Electrochem. Soc. 138 (1991) 349.
[13] S.B. Adler, Chem. Rev. 104 (2004) 4791.
[14] Z.G. Lu, J. Hardy, J. Templeton, J. Stevenson, J. Power Sources 196 (2011) 39.
[15] S.P. Simner, M.D. Anderson, L.R. Pederson, J.W. Stevenson, J. Electrochem. Soc. 152 (2005) A1851.
[16] J.W. Stevenson, T.R. Armstrong, R.D. Carneim, L.R. Pederson, W.J. Weber, J. Electrochem. Soc. 143 (1996) 2722.
[17] C.C. Chen, M.M. Nasrallah, H.U. Anderson, J. Electrochem. Soc. 142 (1995) 491.
[18] L.W. Tai, M.M. Nasrallah, H.U. Anderson, D.M. Sparlin, S.R. Sehlin, Solid State Ionics 76 (1995) 273.